Flow Interaction Between Two Spheres at Moderate Reynolds Number

A. D. Brydon[1] and M. C. Thompson[2]

[1]Department of Mathematics and Statistics
University of New Mexico, NM 87131 U.S.A.

[2]Department of Mechanical Engineering
Monash University, Clayton, Victoria, 3800 AUSTRALIA

Abstract

The flow past two separated spheres placed side-by-side is examined using a fully three-dimensional parallel spectral-element code developed by the first author. Whilst this is primarily a fundamental study, the flow system represents a sub-component of fluid-particle flows and is of importance to the development of physical models describing flows with non-zero particle loadings.

Experimental flow visualisations reveal that the wakes interact strongly at small separations and at least three different wake states can be observed. The numerical results reported here were aimed at accurately simulating the change in the wake state as the separation is decreased. The results are analysed in terms of vorticity generation and interaction, and flow-induced forces on the spheres.

Introduction

The flow past a single sphere is a generic example of more general flows past compact bluff objects. Simulation of the interaction of the wake flows from more than one sphere represents an initial step in producing an understanding of the interactions of more complicated particle laden flows.

Experimental studies of flow past a single sphere (e.g., Provansal and Ormières [9], Johnson and Patel [3]) show at low Reynolds numbers the wake behind the sphere is steady and symmetric. As the Reynolds number (based on free stream velocity and sphere diameter) is increased above $Re = 210$, the wake flow structure changes to an non-axisymmetric, but still steady form. This flow configuration is often referred to as a double-threaded wake, due to the two streams of dye observed from the rear of the object in the experimental visualisations (Margavey and Bishop [6], [7]). These two tails occur off the centreline of the flow, leading to a single plane of symmetry rather than the previous axisymmetric flow pattern.

As the Reynolds number is increased above $Re = 280$, the wake pattern becomes unsteady, with vortex loops or hairpin structures forming in the wake from the sphere. This structure again has a single plane of symmetry.

For a single sphere flow, Johnson and Patel [3] compared finite-difference simulations with experimental results, successfully using the vortex visualization method of Jeong and Hussain [2] to examine the wake vortex structures. The transition from a planar symmetric double-threaded wake to a wake consisting of vortex loops or hairpins is clearly shown.

Tomboulides and Orszag [10] performed a comprehensive series of simulations on single sphere flow up to a Reynolds number of 1000. Their work concluded that the flow undergoes a transition from axisymmetric to steady non-axisymmetric flow at $Re = 212$, and from this state to a single frequency shedding flow at $Re = 270$; numbers in good agreement with earlier experimental results.

The purpose of the current work is to examine the interaction of shedding sphere wakes by placing two spheres side-by-side. A Reynolds number of 300, based on the sphere diameter, is maintained throughout the current work, which is above the critical Reynolds number corresponding to the hairpin shedding wake of the single sphere flow. The experimental work of Leweke *et al.* [5]) shows that the wake structure is dramatically affected by the separation between the spheres. This dramatic change is shown in the experimental dye visualisations of these authors in Figure 1. The corresponding Reynolds number is approximately 350, however, the behaviour is not very sensitive close to this value.
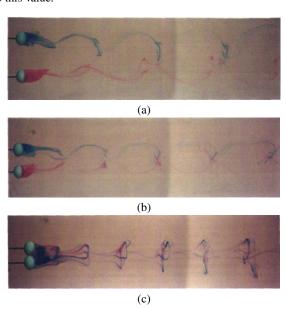

(a)

(b)

(c)

Figure 1: Experimental dye visualisations showing the change in the wake interaction as the separation is decreased. (a) $S/d = 3$, (b) $S/d = 2$, (c) $S/d = 1$, where S/d is the separation in terms of cylinder diameters.

Method

A parallel fully three-dimensional spectral-element method, developed by the first author, is used to simulate the incompressible Navier-Stokes equations at a Reynolds number of 300, based on the inlet velocity and the sphere diameter. The spectral-element method offers the possibility of very high-order spatial descretization of the domain, and is particularly suited to problems with smooth domains and boundary conditions, such as the one under consideration.

The temporal discretization uses the high-order splitting method of Karniadakis *et al.* [4]. By using the high-order pressure boundary conditions of this work, second-order temporal ac-

curacy is achieved.

For the single sphere simulations, the eighth-order spectral element mesh of 676 elements was used to simulate the flow domain, consisting of approximately $360,000$ nodal points. The mesh is carefully concentrated around the sphere and in the near wake flow where the velocity gradients are maximal.

With the flow aligned along the x axis, the domain extends to a distance of $4d$ upstream, and $20d$ downstream, where the sphere diameter is d. The flow domain is truncated with slip boundaries on a square tube at $y, z = \pm 4d$, giving a blockage of around 5%. An inflow velocity of $\mathbf{u} = (U, 0, 0)$ is imposed on the upstream boundary, with zero stress imposed at the outflow boundary.

For the two sphere flow simulations, a second free parameter, S/d, is introduced to specify the non-dimensional distance between the two spheres. The width of the domain in the z direction is extended to $S + 4$ to maintain the distance of each sphere from the boundaries.

The two sphere mesh is similar in structure to the single sphere mesh, with elements added between the two spheres. Because of the increased problem size, the order of elements is reduced to seven. As the distance of the spheres is increased, additional elements are added, so that with $S/d = 1.5$ the mesh contains 1240 elements with approximately $442,000$ nodes, and for $S/d = 2.5$ and 3.5 the mesh contains 1764 elements with approximately $626,000$ nodes.

Full details of the method used, including mesh design and an extensive code validation can be found in Brydon [1].

Results

The results of a steady, planar symmetric, single sphere flow simulation at $Re = 250$ are used to provide the initial condition for the flow at $Re = 300$. The simulation is then evolved forward in time.

Between the non-dimensionalised times $40 \leq (U/d)t \leq 150$, the flow structure changes from a planar symmetric double-threaded wake to the periodic vortex loop wake structure. The time-dependent force on the cylinder gives a single Strouhal frequency of $St = 0.136 \pm 0.0085$ which agrees well with previous numerical results (e.g., Johnson and Patel [3], Tomboulides *et al.* [10]). The average drag coefficient is $C_d = 0.656$, with an average lift coefficient of $C_L = 0.0687$.

Figure 2 shows iso-surfaces of flow quantities for the single sphere flow. The orientation of the wake structure is not enforced by the flow geometry, the results have been rotated to align the planar forces along the y axis, requiring a negative rotation of $42°$ about the x axis.

Figure 2(a) shows the result of applying the vortex visualization method of Jeong and Hussain[2]. This technique defines a vortex as any region with negative eigenvalues of the tensor $\mathbf{S}^2 + \mathbf{\Omega}^2$, where $\mathbf{S}$ and $\mathbf{\Omega}$ represent the local strain and rotation tensors respectively. Since the spectral-element method does not guarantee continuity of derivatives across element boundaries, a small amount of noise is apparent in this vortex quantity relative to the primitive solution variables. This measure of the vortex region does, however, clearly shows the structure of the hairpin vortical wake structure as presented by Johnson and Patel [3].

To simulate the interaction of flow past two side-by-side spheres, the solution from the single sphere flow is used as an initial condition. The use of this flow introduces an initial artificial velocity gradient jump across the plane of symmetry, but
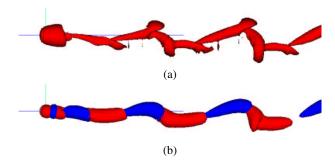

(a)

(b)

Figure 2: Flow past single sphere, $Re = 300$. (a) Iso-surface plot of the vortical wake flow identified by eigenvalue method: side view. (b) Axial vorticity, ω_x: top view. Dark: $\omega = +0.1U/d$, Light: $\omega = -0.1U/d$.

does allow for a significant reduction in the amount of simulation time required to start up the flow.

Figure 3 shows the streamwise force on each of the two spheres at a separation of $S/d = 3.5$. At this separation, the force on each sphere is approximately the same (even over the relatively short simulations times involved), with the shedding from each sphere being similar in magnitude but varying in phase. The second part of the figure shows the angle of the planar forces on each sphere. It is clear that the orientation of the flow is yet to settle down, but it is also clear that the spheres wakes are interacting in a weak fashion. This is also found in the experimental results.
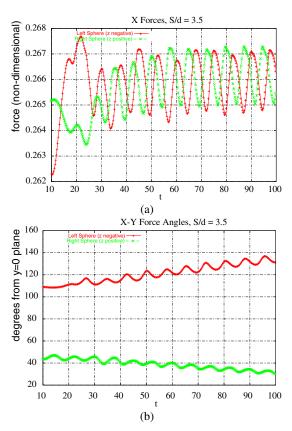

(a)

(b)

Figure 3: Forces on a two spheres at $Re = 300$, $S/d = 3.5$. (a) Axial non-dimensional force. (b) Angle of non-axial forces on sphere.

Figure 4 shows iso-surfaces of the flow quantities for spheres with separation $S/d = 3.5$. The wake is largely unchanged from that seen in the single sphere case. The hairpin structure of the single sphere wake is still present, although the hairpins are not aligned along the axis. By placing the spheres across an axis, a direction is assigned to the wake flow, and it is no longer necessary or appropriate to rotate the wake for visualization.
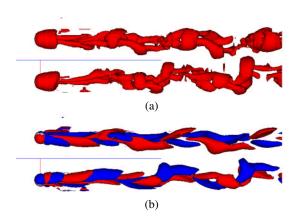

(a)

(b)

Figure 4: Flow past two spheres, $S/d = 3.5$, $Re = 300$. Top view. Contour levels same as Figure 2. (a) Vortical structure in the wake. (b) Axial vorticity, ω_x.

When a sphere separation of $S/d = 2.5$ is started from the single sphere solution, a different configuration is seen in the flow forces of Figure 5. The flow quickly aligns itself along the axis separating the spheres, with significantly smaller forces in the y direction than the z direction. The drag force on each sphere is seen to differ, with the right sphere experiencing a greater drag force. Since the flow configuration is symmetric, it is expected that a direction is chosen arbitrarily, as seen in the single sphere case. The forces on the spheres are also offset by approximately one third of a shedding cycle. The sideways forces on the spheres also indicate that the two spheres repulse each other, although the forces are again out of phase.

Figure 6 shows the lining up of the hairpin structures of the single sphere flow. It seems likely that the one third cycle offset in forces is due to the lining up of these structures. While the individual hairpin structures are seen to form initially, as the flow advects downstream, the loop structures of the two wakes are seen to merge. The vortical structure, shown in part (a) of this figure shows the formation of hairpin vortices, which in the vortex view of the flow remain largely unchanged as the structures travel downstream. The view of streamwise vorticity gives a better indication of the merging of vortex structures in the wake. The lining up of the larger hairpin structures of the right sphere (shown on the bottom) with the smaller hairpin structure of the left sphere is apparent. It is also clear that the vortex structure is not the same for each sphere wake.

Experimental flow visualisations (Leweke *et al.* [5]) indicate that at this separation the wakes interact strongly but the coupling is not complete. Most of the time the wakes face each other with the loop or hairpin structures touching and interacting. Long visualisation records show that occasionally one of the wakes falls out of synchronisation with the other. The recovery to the almost locked state is reasonably rapid compared with the timescale over which the flow remained locked.

When the flow is solved for a separation of $S/d = 1.5$, the forces on the sphere suggest a different flow configuration. The drag force on each sphere is equal, and out of phase by half a cy-
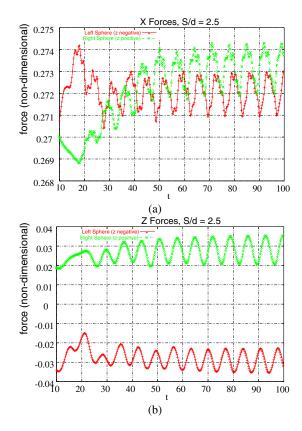

(a)

(b)

Figure 5: Forces on a two spheres at $Re = 300$, $S/d = 2.5$. (a) Axial non-dimensional force. (b) Sideways forces on spheres.
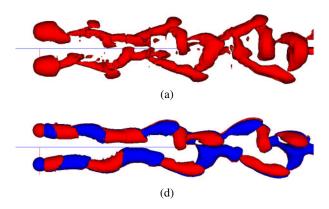

(a)

(d)

Figure 6: Flow past two spheres, $S/d = 2.5$, $Re = 300$. Top view. Contour levels same as Figure 2. (a) Vortical structure in the wake, (b) Axial vorticity, ω_x.

cle. The planar flow forces are again aligned along the x axis separating the two spheres, with the repulsive forces between the spheres increased compared with previous cases. The repulsive forces between the spheres again shows a half cycle phase difference.

At a flow separation of $S/d = 1.5$, the wake structure shows the greatest change. The vortical wake structures, shown in Figure 8(a) is again more complicated, with an outer 'C' shaped vortex region surrounding an inner loop vortex. This outer loop is again apparent in part (b) of the same figure, where the outer parts of the loop are seen to consist of vortex regions of opposing signs.
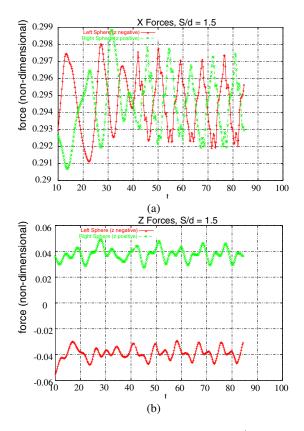
(a)

(b)

Figure 7: Forces on a two spheres at $Re = 300$, $S/d = 1.5$. (a) Axial non-dimensional force. (b) Sideways forces on spheres.
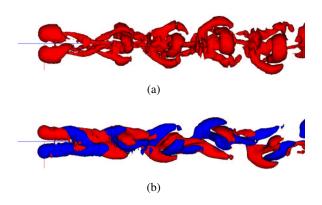

(a)

(b)

Figure 8: Flow past two spheres, $S/d = 1.5$, $Re = 300$. Contour levels same as Figure 2. (a) Vortical wake structure. Top view. (b) Axial vorticity, ω_x. Top view.

Table 1 gives a summary of the various drag and lift coefficients. The single sphere solution is considered equivalent to an infinite separation, where the spheres would have no effect on each other. It is clear that as the spheres are brought closer together, the total drag is increased. When the spheres approach each other, the lift force acts as a repulsion force between the spheres.

Conclusions

This work summarizes the results from full three-dimensional spectral-element simulations of flow past two spheres placed side-by-side at a Reynolds number of 300. It was seen that

S/d	C_d	C_L
1.5	0.75	0.099
2.5	0.69	0.073
3.5	0.67	0.071
∞	0.66	0.069

Table 1: Effect of sphere seperation on drag and lift

as the separation between the spheres is decreased, the flow changes from two largely independent wakes at $S/d = 3.5$ to two aligned wakes with some interaction at $S/d = 2.5$. At this separation the flow is asymmetric, with one sphere experiencing a greater drag force than the other (although this is probably a transient phenomena). As the separation is further reduced to $S/d = 1.5$ the flow features change dramatically, with the force on each sphere becoming symmetric, and a more complicated merges wake structure emerging. Both the experimental and the numerical aspects of this research are continuing to try match parameters more closely, and to understand the interaction in more detail.

References

[1] BRYDON, A., 2001, High-Order Simulation of Swirling and Bluff Body Flows, *Ph.D. thesis*, Department of Mathematics and Statistics, Monash University Melbourne, Australia.

[2] JEONG and HUSSAIN, 1995, On the Identification of a Vortex, *J. Fluid Mech.*, **285**, 69–94

[3] JOHNSON, T.A. & PATEL, V.C. 1999 Flow past a sphere up to a reynolds number of 300. *J. Fluid Mech.* **378**, 19–70

[4] KARNIADAKIS, G., ORSZAG, S. and ISRAELI, M., 1991 High-Order Splitting Methods for the Incompressible Navier-Stokes Equations, *J. Comp. Phys.* **97**, 114.

[5] LEWEKE, Th., ORMIÈRES, D., PROVANSAL, M. and SCHOUVEILER, L., 1999, Visualisations des vortex déversés dans le sillage d'une ou deux sphères, *8th Colloque de Visualisation et de Traitement d'Images en Méchanique des Fluides*, editor P Hébrard, ENSICA, Toulouse, FRANCE, p. 183.

[6] MARGARVEY, R.H. & BISHOP, R.L. 1961a Transition ranges for three-dimensional wakes. *Can. J. Phys.* **39**, 1418–1422

[7] MARGARVEY, R.H. & BISHOP, R.L., 1961b Wakes in liquid-liquid systems. *Phys. Fluids* **4** (7) 800–805.

[8] ORMIÈRES, D. & PROVANSAL, M. 1999a Transition to turbulence in the wake of a sphere. *Phys. Rev. Lett.* **83**, 80–83

[9] PROVANSAL, M. & ORMIÈRES, D. 1998 Etude expérimentale de l'instabilité du sillage d'une sphère. *C. R. Acad. Sci. Paris* **326** (Série II b), 489–494

[10] TOMBOULIDES, A.G., & ORSZAG, S.A. 2000 Numerical investigation of transitional and weak turbulent flow past a sphere. *J. Fluid Mech* **416**, 45–73.